High-Energy Anomaly in the Angle-Resolved Photoemission Spectra of $Nd_{2-x}Ce_xCuO_4$: Evidence for a Matrix Element Effect

E. D. L. Rienks,[1] M. Ärrälä,[2] M. Lindroos,[2] F. Roth,[3] W. Tabis,[4,5] G. Yu,[4] M. Greven,[4] and J. Fink[6,1]
[1]Helmholtz-Zentrum Berlin, Albert-Einstein-Strasse 15, D-12489 Berlin, Germany
[2]Department of Physics, Tampere University of Technology, P.O. Box 692, FIN-33101 Tampere, Finland
[3]Center for Free-Electron Laser Science/DESY, Notkestrasse 85, D-22607 Hamburg, Germany
[4]School of Physics and Astronomy, University of Minnesota, Minneapolis, Minnesota 55455, USA
[5]University of Science and Technology, Faculty of Physics and Applied Computer Science, 30-059 Krakow, Poland
[6]Leibniz-Institute for Solid State and Materials Research Dresden, P.O. Box 270116, D-01171 Dresden, Germany
(Received 18 December 2013; published 23 September 2014)

We use polarization-dependent angle-resolved photoemission spectroscopy (ARPES) to study the high-energy anomaly (HEA) in the dispersion of $Nd_{2-x}Ce_xCuO_4$, $x = 0.123$. We find that at particular photon energies the anomalous, waterfall-like dispersion gives way to a broad, continuous band. This suggests that the HEA is a matrix element effect: it arises due to a suppression of the intensity of the broadened quasiparticle band in a narrow momentum range. We confirm this interpretation experimentally, by showing that the HEA appears when the matrix element is suppressed deliberately by changing the light polarization. Calculations of the matrix element using atomic wave functions and simulation of the ARPES intensity with one-step model calculations provide further evidence for this scenario. The possibility to detect the full quasiparticle dispersion further allows us to extract the high-energy self-energy function near the center and at the edge of the Brillouin zone.

DOI: 10.1103/PhysRevLett.113.137001 PACS numbers: 74.25.Jb, 74.20.-z, 74.72.Ek, 79.60.-i

One of the unique assets of angle-resolved photoemission spectroscopy (ARPES) is the ability to determine the spectral function $A(\omega, \boldsymbol{k})$ in energy and momentum space. The finite width and deviation of the dispersion from that calculated in an independent particle model are interpreted in the majority of cases in terms of many-body effects [1]. In the cuprate high-T_c superconductors, various kinks in the dispersion have been discovered and analyzed in terms of a coupling of the charge carriers to bosonic excitations possibly mediating high-T_c superconductivity in these materials. Besides the kinks in the low binding energy (E_B) region ($E_B \leq 0.1$ eV) a further apparent renormalization has been observed at $E_B = E_H \gtrapprox 0.3$ eV. Here the band appears to bend sharply and seems to proceed almost vertically towards the valence bands. This phenomenon has been termed "waterfall" or high-energy anomaly (HEA) [2]. The HEA has been observed in undoped cuprates [3] as well as in their hole-doped [2,4–13] and electron-doped derivatives [4,13–15]. In the doped compounds E_H shows a d-wave momentum dependence that is larger along the nodal direction and smaller near the antinodal point opposite to the momentum dependence of the d-wave superconducting gap [6,12,14]. The values of E_H exhibit a difference of $\approx$0.4 eV between hole-doped and electron-doped cuprates [4]. This difference was interpreted in terms of a shift of the chemical potential [14]. The experimental studies were accompanied by numerous theoretical papers [16–31].

For the HEA phenomenon, a number of explanations have been suggested including Mott-Hubbard models with a transition from the coherent quasiparticle dispersion to the incoherent lower Hubbard band [5,18,21,26,32], a disintegration of the low-energy branch into a holon and spinon band due to a spin charge separation [2], a coupling to spin fluctuations [9,17,19,29,33], a coupling to phonons [7], string excitations of spin polarons [32], a bifurcation of the quasiparticle band due to an excitation of a bosonic mode of charge $2e$ [22], and a coupling to plasmons [16]. These are all intrinsic interpretations in terms of many-body interactions leading to a change of the spectral function.

However, the spectral function can strictly only be inferred from ARPES with a detailed knowledge of the photoexcitation matrix element, since the measured photocurrent is given by [1]

$$I(\omega, \boldsymbol{k}) \propto |M(\omega, \boldsymbol{k})|^2 A(\omega, \boldsymbol{k}), \tag{1}$$

where the matrix element

$$M(\omega, \boldsymbol{k}) = \langle f | \mathbf{e} \cdot \mathbf{r} | i \rangle \tag{2}$$

is determined by the final state $\langle f|$, the initial state $|i\rangle$, and the dipole operator $\mathbf{e}\cdot\mathbf{r}$ ($\mathbf{e}$ is the unit vector along the polarization direction of the photons).

Some ARPES studies pointed out that extrinsic effects due to matrix element effects may explain the HEA [8,10,12], since changes of the waterfall-like dispersion to a Y-shaped dispersion have been observed upon photon energy variation or by changing the Brillouin zone (BZ). Thereupon, a combination of extrinsic and intrinsic effects has been invoked to explain the ARPES results of cuprates at high energies [11,13,33].

In this Letter we address the controversy regarding the interpretation of the HEA in terms of extrinsic or intrinsic effects. We present a polarization and photon energy dependent ARPES study on the electron-doped cuprate [34] $Nd_{2-x}Ce_xCuO_4$, $x = 0.123$ in several BZs. We find that the waterfall-like dispersion transforms into a normal, dispersive band at certain photon energies. In addition, a waterfall-like dispersion can be induced in the intact band by changing the polarization of the incoming photons. The results can be explained in terms of a wipeout of the intensity of the broadened quasiparticle band in a particular momentum range. Thus, we give strong evidence that the HEA is not caused by intrinsic many-body effects, but rather by extrinsic matrix element effects. Furthermore, the newfound ability to observe the dispersion throughout the entire BZ allows us to determine the mass renormalization of the quasiparticle band relative to density functional theory (DFT) calculations.

The $Nd_{2-x}Ce_xCuO_4$, $x = 0.123$ single crystal was grown in about 4 atm of oxygen using the traveling-solvent floating-zone technique, annealed for 10 h in argon at 970 °C followed by 20 h in oxygen at 500 °C [35]. The sample was antiferromagnetic with a Néel temperature of about $T_N = 82$ K [36]. ARPES measurements were carried out at the synchrotron radiation facility BESSY II using the UE112-PGM2a variable photon polarization beam line and the "1^2"-ARPES end station equipped with a Scienta R8000 analyzer. All measurements were performed at $T = 50$ K. The total energy resolution was set between 10 and 15 meV, while the angular resolution was ≈0.2°. We point out that the ARPES experiments were performed at relatively high photon energies ($h\nu = 50$ to 120 eV), a range in which the cross section for Cu $3d$ state excitations is 5 to 7 times larger than that for O $2p$ states [37]. The crystal was mounted on a six-axis cryomanipulator allowing polar, azimuthal, and tilt rotation of the sample in ultrahigh vacuum with a precision of 0.1°. The experimental geometry is shown in Fig. 1(a). The mirror plane $(0, 0, \pi) - \Gamma - (\pi, 0, 0) \hat{=} (x, 0, z)$ was turned into the scattering plane. In this way, cuts shown in Fig. 1(b) parallel to the $\Gamma - (0, \pi)$ direction for various k_x values could be recorded by changing the polar angle from nearly normal incidence to more grazing incidence. In the chosen sample orientation, the Cu $3d_{x^2-y^2}$ conduction band states have an even symmetry with respect to the scattering plane as shown in Fig. 1(a). For nonzero photoemission intensity on the mirror plane, the final state must be even with respect to this plane and the same holds for the product of the dipole operator and the initial state. Therefore, for this sample orientation and for p-polarized light (**e** parallel to the mirror plane, dipole operator even) the matrix element should be finite near the mirror plane, while for s-polarized light (**e** perpendicular to the mirror plane, dipole operator odd) the matrix element should vanish [see Eq. (2)]. In a study of the origin of the shadow Fermi surface in cuprates it was shown that the intensity vanishes in a narrow range of ±2° when the transition is symmetry forbidden [38].

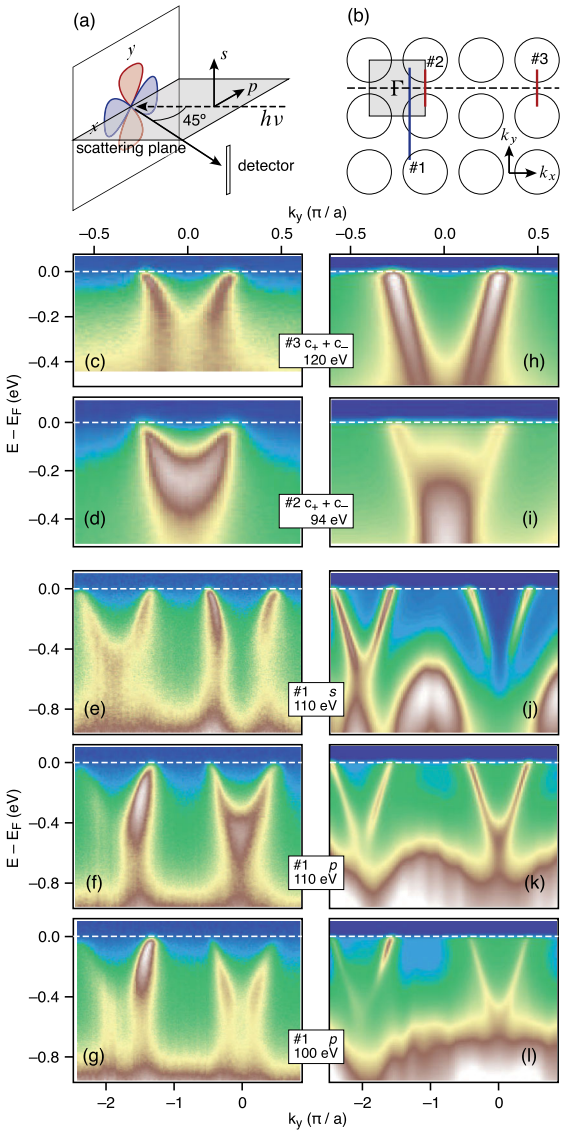

FIG. 1 (color online). (a) Experimental geometry. (b) Cuts in the reciprocal space used in the present investigation. (c)–(g) Experimental ARPES intensity distribution maps recorded with parameters given in the labels. (h)–(l) calculated ARPES intensities using the parameters of (c)–(g), respectively. For both the ARPES data and the calculations linear intensity scales with arbitrary scales were used.

ARPES intensity calculations were done fully relativistically based on the Dirac equation [39]. One-step model [40] and multiple scattering theory were utilized. The latter also was used for the final states. The potential for Nd_2CuO_4 was calculated by using self-consistent electronic structure calculations with the Korringa-Kohn-Rostoker method [41,42]. In the calculations, many-body correlations were taken into account by the complex self-energy function Σ. For the initial state we used the

experimental self-energy function derived from the ARPES experiments (see below). For the final state a constant value $\Im\Sigma_f = 2$ eV was used.

In Figs. 1(c) and 1(d) we present the sum of ARPES intensity plots along the BZ edges recorded with right (c_+) and left (c_-) circularly polarized photons having two different photon energies. For $h\nu = 120$ eV [see Fig. 1(c)] and $k_x = 5\pi$ [cut No. 3 in Fig. 1(b)] a clear HEA at $E_H = 0.25$ eV is detected. At this energy the normal dispersion transforms into a vertical waterfall-like dispersion accompanied by a reduction of the intensity near $k_y = 0$. On the other hand, changing the photon energy to $h\nu = 94$ eV [see Fig. 1(d)] and $k_x = \pi$ [cut No. 2 in Fig. 1(b)] reveals a band with a normal dispersion and with a width at constant energy that continuously increases with increasing binding energy. Since we observe similar changes as a function of photon energy for $k_x = n\pi$, $n = 1, 3$, and 5 (not shown) we conclude that the change of the spectra shown in Figs. 1(c) and 1(d) is caused by the variation of the photon energy and not by the change of k_x. Furthermore, $Nd_{2-x}Ce_xCuO_4$ is essentially a two-dimensional electronic system [43]. Therefore, while $k_\perp$ changes upon variation of the photon energy, this is not expected to change the spectral function. Thus, the drastic change of the intensity plots presented in Figs. 1(c) and 1(d) indicates that the HEA is caused by matrix element effects and not by changes of the spectral function.

In Figs. 1(e)–1(g) we present similar energy distribution maps, but now recorded with the wave vectors $k_x = 3\pi/8$ [cut No. 1 in Fig. 1(b)]. In these cuts, the Fermi surface is crossed at the nodal point. For $h\nu = 110$ eV and p polarization, a normal dispersion is observed near $k_y = 0$ [see Fig. 1(f)]. Compared to the antinodal point, the bottom of the band has moved to higher E_B, which is expected from band structure calculations. The spectral weight of the band extends into the region of the nonbonding oxygen valence bands. On the other hand, near $k_y = -2\pi$, a HEA is observed. At the same photon energy ($h\nu = 110$ eV) but for s polarization, we know that the intensity must vanish at the mirror plane ($k_y = 0$). In Fig. 1(e) we see that, when the matrix element is intentionally suppressed in this way, a HEA appears at $E_H = 0.4$ eV. Thus, the existence of the waterfall-like dispersion can be unambiguously attributed to a vanishing matrix element near $k_y = 0$. In the second BZ we detect a more normal dispersion. Furthermore, for $h\nu = 100$ eV and p polarization, a HEA is observed in the first and the second BZ [see Fig. 1(g)]. Comparing the spectra presented in Figs. 1(f) and 1(g) which both were measured with the same (p) polarization, the difference near $k_y = 0$ cannot be explained by a suppression of the matrix element due to a specific photon polarization but rather indicates an extinction of the matrix element near the (k_x, $k_y = 0$) line for specific photon energies. Comparing the intensities near $k_y = 0$ presented in Figs. 1(e) and 1(g), it is remarkable that the distances between the waterfall-like

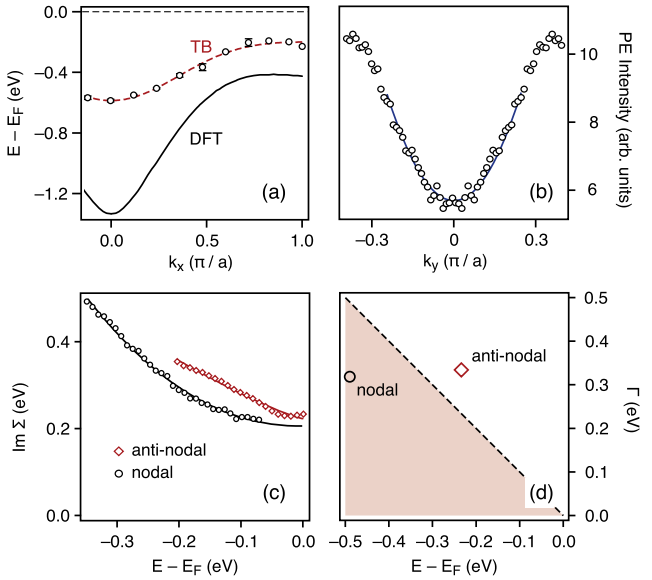

FIG. 2 (color online). (a) Bottom of the band along the $(-\pi, 0)$–$(\pi, 0)$ direction between the center of the BZ and the antinodal point. Circles: ARPES data. Dashed line: tight binding (TB) fit. Solid line: present density functional theory (DFT) calculations. (b) Momentum distribution curve of the data shown in Fig. 1(e) at $E_B = 0.5$ eV, symmetrized relative to $k_y = 0$. The blue line shows a quadratic momentum dependence. (c) Imaginary part of the self-energy $\Im\Sigma$ as a function of the binding energy near the nodal and the antinodal point. The lines are fits to the data (see text). (d) Width Γ of the spectral weight at the bottom of the band near the antinodal point [$k_\parallel = (\pi, 0)$] and at the cut through the nodal point [$k_\parallel = (3\pi/8, 0)$]. Red region indicates the range of the existence of quasiparticles ($\Gamma < E_B$).

dispersions in momentum space along k_y is about twice as large for the former than for the latter. We attribute the differences in E_H (changing from 0.4 to 0.55 eV) to the different extinction ranges of the matrix elements. In Fig. 2(a) we plot the bottom of the band along the $\Gamma - (\pi, 0)$ direction, derived from fits of energy distribution curves at $k_y = 0$ using spectra that show no HEA and compare this result with our DFT calculations.

The interpretation of the ARPES results on the HEA in terms of matrix element effects is supported by a simple calculation of the matrix element for the selected geometry and sample orientation using atomic wave functions for the $|d\rangle$ initial state and $\langle p|/\langle f|$ final states [44]. As expected, these calculations yield for s-polarization a vanishing matrix element at the mirror plane, but for photons emitted at a finite angle relative to the mirror plane the matrix element increases linearly with that angle. This means that for small angles the intensity should increase proportionally to k_y^2 which is in perfect agreement with a momentum distribution curve at $E_B = 0.5$ eV of the ARPES data shown in Fig. 1(e) [see Fig. 2(b)]. One explanation to account for the observed $h\nu$ dependence would be that for particular photon energies only final states that are odd with

respect to the mirror plane can be reached. This would explain why for p polarization the intensity is zero in the mirror plane. The calculation predicts for finite emission angles relative to the mirror plane a finite intensity proportional to k_y^2 due to even final states that contribute to the matrix element linearly with increasing angle. This would explain why for certain energies even for p polarization a waterfall-like dispersion is observed [see Fig. 1(g)].

The interpretation of the HEA in terms of extrinsic matrix element effects is furthermore strongly supported by the ARPES intensity calculations that are in qualitative agreement with the experimental ARPES data [see Figs. 1(h)–1(l))]. Part of the remaining differences are related to the fact that for the nonbonding O $2p$ bands, the same self-energy function as for the Cu $3d$ band has been used, which leads to an unphysical broadening of the former bands.

The presented ARPES data together with the supporting calculations provide strong evidence that the HEA is not related to an anomalous spectral function, i.e., to specific many-body effects. Rather, it is caused by a wipeout of a broad intensity distribution of the spectral weight near particular high-symmetry lines due to the extinction of the matrix elements (see also Fig. 2 in the Supplemental Material [44]), i.e., by extrinsic effects.

We point out that there are two prerequisites for the appearance of the waterfall-like dispersion in $Nd_{2-x}Ce_xCuO_4$: (i) a locally vanishing matrix element and (ii) a strong broadening of the spectral weight at higher binding energies. As a consequence, the HEA can occur in other strongly correlated systems with a strong broadening of the "bands" with increasing binding energy due to high scattering rates.

In fact, we argue that extrinsic effects underlie the HEA in the hole-doped cuprates as well. The basis for this assertion is the observation of a Y-shaped (instead of a waterfall-like) dispersion for certain measurement geometries in $Bi_2Sr_2CaCu_2O_8$ [8]. The dispersion shown in that work is very similar to the one we present in Fig. 1(f). The observation of a dispersion without anomaly would exclude an intrinsic origin. A further indication that the situation is the same in p- and n-doped systems is provided by the momentum dependence of E_H. In both hole-[6] and electron-doped [14] systems, E_H is found to decrease going from the nodal towards the antinodal point. This effect can be readily explained in terms of a suppression of the intensity of a normal quasiparticle band: near Γ the bottom of the band is deeper than at the antinodal point. It, therefore, intersects the wipeout region at a higher binding energy. Furthermore, the difference of the E_H values of $\approx$0.4 eV between p- and n-doped cuprates, which was linked to the difference of the chemical potential [14] can now be understood as a wipeout of quasiparticle bands, ranging to different energies below the Fermi level. Finally, the angular width of the wipeout region at the antinodal point in $Nd_{2-x}Ce_xCuO_4$ is comparable to that observed in p-type doped $Bi_2Sr_2CaCu_2O_8$ [38].

Since we can now follow the dispersion to the bottom of the band, we can derive reliable results for the mass enhancement compared to DFT calculations. Using the data presented in Fig. 2(a), we obtain a high-energy mass renormalization of 2.1 near the antinodal point while at Γ a value of 2.3 derived. We remark that these values have large errors of about 30% as a result of the considerable variation in the energy of the Cu-O conduction band relative to the Fermi level in the published DFT calculations. Moreover, we have analyzed the energy dependence of the imaginary part of the self-energy, extracted from momentum distribution curves, using the relation $\Im\Sigma = -A - BE^{\alpha}$ [see Fig. 2(c)]. Near the antinodal point we obtain $A = 0.111 \pm 0.003$ eV, $B = 0.47 \pm 0.09$ eV$^{1-\alpha}$, and $\alpha = 1.2 \pm 0.1$, whereas near the nodal point $A = 0.103 \pm 0.002$ eV, $B = 1.4 \pm 0.1$ eV$^{1-\alpha}$, and $\alpha = 2.15 \pm 0.07$. The observation of a nearly quadratic increase as a function of energy at the nodal point indicates a Fermi liquid behavior and explains the quadratic temperature dependence of the in-plane resistivity above the superconducting transition temperature [45]. The nearly linear increase at the antinodal point signals the proximity to a marginal Fermi liquid [46]. Near the center of the BZ, at $k_{\parallel} = (3\pi/8, 0)$ the total lifetime broadening amounts to 65% of E_B [see Fig. 2(d)]. This indicates that even at the bottom of the band, spectral weight of quasiparticles is observed and that at these E_B values we are not in the incoherent range as previously suggested in the literature [5,18,21,26,32]. In addition, the lack of a high-energy kink and the continuous increase of the width as a function of E_B do not support scenarios of a strong coupling of the charge carriers to discrete high-energy bosonic excitations such as magnetic excitations with an energy of $2J \approx 0.3$ eV (J is the exchange energy) [34] which could mediate high-T_c superconductivity [9,17,19,29,33]. Rather, the results presented here indicate a strong coupling of the charge carriers to low-energy electronic excitations, e.g., spin excitations between regions near the antinodal points leading there to a marginal Fermi liquid behavior as described by [47,48].

To summarize, our ARPES results on an n-doped cuprate together with a calculation of the ARPES intensity in a one-step model clearly show that the HEA is not related to an intrinsic anomalous dispersion of the spectral weight. Rather, it is caused by a combination of a wipeout due to matrix element effects and high scattering rates at high energies. By selecting suitable photon energies we are able to obtain important information on the many-body properties of doped cuprates which places strong constraints on theories of high-T_c superconductivity in these systems. Furthermore, the present results provide important information about the electronic structure of doped Mott-Hubbard insulators: a vertical dispersion between the

coherent quasiparticles and the incoherent lower Hubbard band [5,18,21,26,32] is not supported.

We thank Inna Vishik for valuable comments. The work at the University of Minnesota was supported by the NSF and the NSF MRSEC program.

[1] A. Damascelli, Z. Hussain, and Z.-X. Shen, Rev. Mod. Phys. **75**, 473 (2003).
[2] J. Graf *et al.*, Phys. Rev. Lett. **98**, 067004 (2007).
[3] F. Ronning, K. Shen, N. Armitage, A. Damascelli, D. Lu, Z.-X. Shen, L. Miller, and C. Kim, Phys. Rev. B **71**, 094518 (2005).
[4] Z.-H. Pan *et al.*, arXiv:cond-mat/0610442.
[5] W. Meevasana *et al.*, Phys. Rev. B **75**, 174506 (2007).
[6] J. Chang *et al.*, Phys. Rev. B **75**, 224508 (2007).
[7] B. P. Xie *et al.*, Phys. Rev. Lett. **98**, 147001 (2007).
[8] D. S. Inosov *et al.*, Phys. Rev. Lett. **99**, 237002 (2007).
[9] T. Valla, T. Kidd, W.-G. Yin, G. Gu, P. Johnson, Z.-H. Pan, and A. Fedorov, Phys. Rev. Lett. **98**, 167003 (2007).
[10] D. S. Inosov *et al.*, Phys. Rev. B **77**, 212504 (2008).
[11] W. Meevasana, F. Baumberger, K. Tanaka, F. Schmitt, W. Dunkel, D. Lu, S.-K. Mo, H. Eisaki, and Z.-X. Shen, Phys. Rev. B **77**, 104506 (2008).
[12] W. Zhang *et al.*, Phys. Rev. Lett. **101**, 017002 (2008).
[13] B. Moritz *et al.*, New J. Phys. **11**, 093020 (2009).
[14] M. Ikeda, T. Yoshida, A. Fujimori, M. Kubota, K. Ono, Y. Kaga, T. Sasagawa, and H. Takagi, Phys. Rev. B **80**, 184506 (2009).
[15] F. Schmitt *et al.*, Phys. Rev. B **83**, 195123 (2011).
[16] R. S. Markiewicz and A. Bansil, Phys. Rev. B **75**, 020508 (R) (2007).
[17] R. S. Markiewicz, S. Sahrakorpi, and A. Bansil, Phys. Rev. B **76**, 174514 (2007).
[18] K. Byczuk, M. Kollar, K. Held, Y.-F. Yang, I. A. Nekrasov, Th. Pruschke, and D. Vollhardt, Nat. Phys. **3**, 168 (2007).
[19] A. Macridin, M. Jarrell, T. Maier, and D. J. Scalapino, Phys. Rev. Lett. **99**, 237001 (2007).
[20] P. Srivastava, S. Ghosh, and A. Singh, Phys. Rev. B **76**, 184435 (2007).
[21] F. Tan, Y. Wan, and Q.-H. Wang, Phys. Rev. B **76**, 054505 (2007).
[22] R. G. Leigh, P. Phillips, and T.-P. Choy, Phys. Rev. Lett. **99**, 046404 (2007).
[23] L. Zhu, V. Aji, A. Shekhter, and C. M. Varma, Phys. Rev. Lett. **100**, 057001 (2008).
[24] P. Wrobel, W. Suleja, and R. Eder, Phys. Rev. B **78**, 064501 (2008).
[25] C. Weber, K. Haule, and G. Kotliar, Phys. Rev. B **78**, 134519 (2008).
[26] M. M. Zemljic, P. Prelovsek, and T. Tohyama, Phys. Rev. Lett. **100**, 036402 (2008).
[27] K. Matho, J. Electron Spectrosc. Relat. Phenom. **181**, 2 (2010).
[28] S. Sakai, Y. Motome, and M. Imada, Phys. Rev. B **82**, 134505 (2010).
[29] R. Markiewicz, T. Das, S. Basak, and A. Bansil, J. Electron Spectrosc. Relat. Phenom. **181**, 23 (2010).
[30] B. Moritz, S. Johnston, and T. Devereaux, J. Electron Spectrosc. Relat. Phenom. **181**, 31 (2010).
[31] D. Katagiri, K. Seki, R. Eder, and Y. Ohta, Phys. Rev. B **83**, 165124 (2011).
[32] E. Manousakis, Phys. Rev. B **75**, 035106 (2007).
[33] S. Basak, T. Das, H. Lin, J. Nieminen, M. Lindroos, R. S. Markiewicz, and A. Bansil, Phys. Rev. B **80**, 214520 (2009).
[34] N. P. Armitage, P. Fournier, and R. L. Greene, Rev. Mod. Phys. **82**, 2421 (2010).
[35] P. K. Mang, S. Larochelle, A. Mehta, O. Vajk, A. Erickson, L. Lu, W. Buyers, A. Marshall, K. Prokes, and M. Greven, Phys. Rev. B **70**, 094507 (2004).
[36] E. M. Motoyama, G. Yu, I. M. Vishik, O. P. Vajk, P. K. Mang, and M. Greven, Nature (London) **445**, 186 (2007).
[37] J. Yeh and I. Lindau, At. Data Nucl. Data Tables **32**, 1 (1985).
[38] A. Mans *et al.*, Phys. Rev. Lett. **96**, 107007 (2006).
[39] J. Braun, Rep. Prog. Phys. **59**, 1267 (1996).
[40] J. Pendry, Surf. Sci. **57**, 679 (1976).
[41] S. Kaprzyk and A. Bansil, Phys. Rev. B **42**, 7358 (1990).
[42] A. Bansil, S. Kaprzyk, P. E. Mijnarends, and J. Toboła, Phys. Rev. B **60**, 13396 (1999).
[43] S. Massidda, N. Hamada, J. Yu, and A. Freeman, Physica (Amsterdam) **157C**, 571 (1989).
[44] See Supplemental Material at http://link.aps.org/supplemental/10.1103/PhysRevLett.113.137001 for a calculation of the angle dependent matrix element assuming atomic initial and final states.
[45] C. Tsuei, A. Gupta, and G. Koren, Physica (Amsterdam) **161C**, 415 (1989).
[46] C. Varma, Z. Nussinov, and W. van Saarloos, Phys. Rep. **361**, 267 (2002).
[47] P. Monthoux, A. V. Balatsky, and D. Pines, Phys. Rev. Lett. **67**, 3448 (1991).
[48] A. Abanov, A. V. Chubukov, and J. Schmalian, Adv. Phys. **52**, 119 (2003).